Progress In Electromagnetics Research C, Vol. 113, 47–58, 2021

Radiation of Electromagnetic Waves by an Arbitrarily Oriented Slot at the End Wall of a Rectangular Waveguide

Mikhail V. Nesterenko*, Victor A. Katrich, Victor I. Kijko, and Svetlana V. Pshenichnaya

Abstract—A problem of electromagnetic waves radiation diffracted at a narrow rectilinear arbitrarily oriented slot cut in an end wall of a semi-infinite rectangular waveguide is solved by an asymptotic averaging method. The slot radiates into a half-space over an infinite perfectly conducting plane. An influence of slot inclination angle upon energy and spatial characteristics is numerically studied. Theoretical results are compared with experimental data. A numerical-analytical problem of a narrow rectilinear slot radiating into the space above an infinite impedance plane is also presented. The asymptotic solution for the slot magnetic current was obtained by a generalized method of induced magnetomotive forces (MMF) by using Green's functions of a space above the impedance plane. The effect of the plane with impedance coating on the slot is reduced taking into account an additional term to the slot external conductivity, for which the expressions were obtained in an analytical form.

1. INTRODUCTION

At the present time, narrow slots cut in rectangular waveguide end walls whose longitudinal axis is parallel to one of the coordinate system axes are widely used in microwave antenna-waveguide technology. The slots can serve as radiators which radiate into a half-space above an infinite screen [1–3], as coupling elements between various electrodynamic volumes [4–6] and as structural components of combined radiating structures [7]. A control of electrodynamic characteristics of the radiators and coupling slots can be realized, first of all, by varying slot geometric dimensions and positions relative to the waveguide walls under conditions that the coordinate system axes associated with the slot and waveguide are parallel. One of the ways to achieve required frequency-energy and spatial characteristics of slot radiators consists in varying an inclination angle of a longitudinal slot axis relative to coordinate waveguide axes [8–12]. In this case, the single slot cut in the waveguide end wall, in contrast to the one located on its side walls, can radiate up to 100% of the supplied power.

In this paper, the problem of electromagnetic wave radiation into a half-space above an infinite perfectly conducting plane by a narrow rectilinear inclined slot cut in the end wall of a semi-infinite rectangular waveguide is solved in a strict self-consistent formulation. The obtained approximate analytical expressions were applied to studying energy and spatial field characteristics of the structure in near and far zone. The approximate analytical expressions obtained by this approach have allowed us to find energy and spatial characteristics of the structures. A technique of numerical-analytical solution of the problem concerning radiation by the narrow rectilinear slot into space above the infinite plane, characterized by a distributed surface impedance, is also presented. This approach makes it possible to use solutions obtained for slots radiating into space above perfectly conducting planes as basis functions.

Received 23 April 2021, Accepted 24 May 2021, Scheduled 1 June 2021

* Corresponding author: Mikhail V. Nesterenko (mikhail.v.nesterenko@gmail.com).

The authors are with the Department of Radiophysics, Biomedical Electronics and Computer Systems, V. N. Karazin Kharkiv National University, 4, Svobody Sq., Kharkiv 61022, Ukraine.

2. PROBLEM FORMULATION AND SOLUTION

Consider the waveguide-slot structure shown in Fig. 1. The narrow rectilinear slot is cut in the end wall of the semi-infinite rectangular waveguide whose cross-section is $\{a \times b\}$. The slot length $2L$ and width d satisfy the following inequalities $d/(2L) \ll 1$, $d/\lambda \ll 1$ (λ is the wavelength in free space). The angle between the longitudinal slot axis $\{0s\}$ and the axis $\{0x\}$ of the Cartesian coordinate system associated with the waveguide cross-section is φ. The coordinates of the slot center are $(a/2, y_0, 0)$.

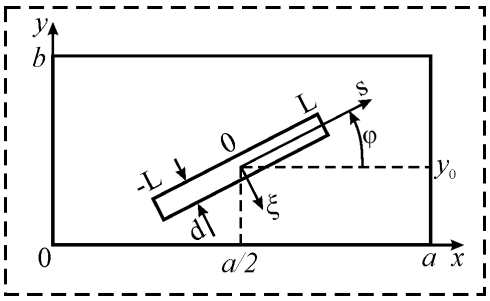

Figure 1. The radiation structure geometry and accepted notations.

Let fields and currents depend on time as $e^{i\omega t}$ (t is the time, and ω is the angular frequency). Under condition $|\xi - \xi'| \approx d/4$ (ξ, (ξ') are local transverse coordinates), the equivalent magnetic current $J(s)$ in the coupling slot between the two electrodynamic volumes satisfies the following quasi-one-dimensional integral equation [13]

$$\left(\frac{d^2}{ds^2} + k^2\right) \int_{-L}^{L} J(s') \left[G_s^{Wg}(d; s, s') + G_s^{Hs}(d; s, s')\right] ds' = -i\omega H_{0s}(s) \tag{1}$$

where $k = 2\pi/\lambda$, G_s^{Wg}, and G_s^{Hs} are the s-components of magnetic tensor Green's functions for the vector Hertz potentials for a semi-infinite rectangular waveguide (index Wg) and half-space (index Hs); $H_{0s}(s)$ is the projection of magnetic fields of external sources on the slot axis.

In general form, i.e., when the exciting field and slot location are not specified, the solution of Equation (1) can be obtained by the asymptotic averaging method after introducing a natural small parameter $\alpha = 1/(8\ln(d/(8L)))$ [13]

$$J(s) = \bar{A}(-L)\cos ks + \bar{B}(-L)\sin ks + \alpha \int_{-L}^{s} \left\{\frac{i\omega}{k} H_{0s}(s') + \bar{F}_N[s', \bar{A}, \bar{B}]\right\} \sin k(s - s') ds', \tag{2}$$

where

$$\begin{aligned} \bar{F}_N[s, \bar{A}, \bar{B}] \;=\; & \left[\bar{A}(+L)\sin kL - \bar{B}(+L)\cos kL\right] G_s^{\Sigma}(s, L) \\ & + \left[\bar{A}(-L)\sin kL + \bar{B}(-L)\cos kL\right] G_s^{\Sigma}(s, -L) \end{aligned} \tag{3}$$

is the averaged slot eigenfield, $G_s^{\Sigma}(s, s') = G_s^{Wg}(d; s, s') + G_s^{Hs}(d; s, s')$; $\bar{A}(\pm L)$ and $\bar{B}(\pm L)$ are the arbitrary constants which are defined by the slot excitation method and slot position relative to the waveguide walls. Assuming that the H_{10}-wave propagates in the waveguide from the direction $z = -\infty$, the following expression can be written

$$H_{0s}(s) = 2H_0 \cos\varphi \cos \tilde{k}s, \quad \tilde{k} = (\pi/a)\cos\varphi, \tag{4}$$

where H_0 is the incident field amplitude. When the constants $\bar{A}(\pm L)$ and $\bar{B}(\pm L)$ are defined using the expressions (4), geometry structure, and boundary conditions for the current $J(\pm L) = 0$, the final expression for current can be written as

$$J(s) = -\alpha 2H_0 \cos\varphi \left(\frac{i\omega}{k^2}\right) \frac{2\sin kL \left(\cos ks \cos \tilde{k}L - \cos kL \cos \tilde{k}s\right)}{\left[1 - (\tilde{k}/k)^2\right] \{\sin 2kL + \alpha\left[2P_0(kd, 2kL) + W_0(kd, 2kL)\right]\}}. \tag{5}$$

In Equation (5), $P_0(kd, 2kL)$ and $W_0(kd, 2kL)$ are the functions of the slot eigenfield determined by the corresponding components of the Green's functions which according to Eq. (3) are equal

$$\begin{aligned} P_0(kd,2kL) &= \sin 2kL[Cc_i(kd,2kL) - iSc(kd,2kL)] \\ &\quad +(1-\cos 2kL)[Cs(kd,2kL) - iSs(kd,2kL)], \end{aligned} \tag{6a}$$

$$\begin{aligned} W_0(kd_e,2kL) &= \frac{4\pi}{ab}\sum_{m=0}^{\infty}\sum_{n=0}^{\infty}\frac{\varepsilon_m\varepsilon_n}{k_z}\Bigg\langle \cos^2\varphi\Bigg\{ \sin kL\Bigg[\Phi_s(k_x x_0)\Phi_c(k_y y_0)(\cos k_1 L + \cos k_2 L)I_1^+(k_{1,2}L) \\ &\quad +\Phi_c(k_x x_0)\Phi_s(k_y y_0)(\cos k_1 L - \cos k_2 L)I_1^-(k_{1,2}L)\Bigg] \\ &\quad +\frac{1}{2}\cos kL \sin 2k_y y_0\Bigg[\Phi_s(k_x x_0)(\cos k_1 L + \cos k_2 L)I_2^-(k_{1,2}L) \\ &\quad -\Phi_c(k_x x_0)(\cos k_1 L - \cos k_2 L)I_2^+(k_{1,2}L)\Bigg]\Bigg\} \\ &\quad +\sin^2\varphi\Bigg\{ \sin kL\Bigg[\Phi_s(k_x x_0)\Phi_c(k_y y_0)(\cos k_1 L - \cos k_2 L)I_1^-(k_{1,2}L) \\ &\quad +\Phi_c(k_x x_0)\Phi_s(k_y y_0)(\cos k_1 L + \cos k_2 L)I_1^+(k_{1,2}L)\Bigg] \\ &\quad +\frac{1}{2}\cos kL \sin 2k_y y_0\Bigg[\Phi_s(k_x x_0)(\cos k_1 L - \cos k_2 L)I_2^+(k_{1,2}L) \\ &\quad -\Phi_c(k_x x_0)(\cos k_1 L + \cos k_2 L)I_2^-(k_{1,2}L)\Bigg]\Bigg\}\Bigg\rangle. \end{aligned} \tag{6b}$$

In formulas (6), the following notations are adopted:

$$I_1(k_{1,2}L) = \frac{k\sin kL\cos k_{1,2}L - k_{1,2}\cos kL\sin k_{1,2}L}{k^2 - k_{1,2}^2},$$

$$I_2(k_{1,2}L) = \frac{k_{1,2}\sin kL\cos k_{1,2}L - k\cos kL\sin k_{1,2}L}{k^2 - k_{1,2}^2},$$

$$\Phi_{\left\{\begin{smallmatrix}s\\c\end{smallmatrix}\right\}}(k_x x_0) = \left\{\begin{array}{c}\sin(k_x x_0^{\varphi})\\ \cos(k_x x_0^{\varphi})\end{array}\right\}\times\left\{\begin{array}{c}\sin(k_x x_0)\\ \cos(k_x x_0)\end{array}\right\}, \quad \Phi_{\left\{\begin{smallmatrix}s\\c\end{smallmatrix}\right\}}(k_y y_0) = \left\{\begin{array}{c}\sin(k_y y_0^{\varphi})\\ \cos(k_y y_0^{\varphi})\end{array}\right\}\times\left\{\begin{array}{c}\sin(k_y y_0)\\ \cos(k_y y_0)\end{array}\right\},$$

$I_{1,2}^{\pm}(k_{1,2}L) = I_{1,2}(k_1 L) \pm I_{1,2}(k_2 L)$; $k_{1,2} = k_x\cos\varphi \pm k_y\sin\varphi$; $x_0^{\varphi} = (a/2) - (d/4)\sin\varphi$; $y_0^{\varphi} = y_0 + (d/4)\cos\varphi$, $\varepsilon_{m,n} = 1$ if $m,n = 0$, $\varepsilon_{m,n} = 2$ if $m,n \neq 0$, $k_x = m\pi/a$, $k_y = n\pi/b$ (m,n are integers), $k_z = \sqrt{k_x^2 + k_y^2 - k^2}$, and Cc_i, Sc, Cs, Ss are generalized integral functions related to the integral sine Si and cosine Cin [14]:

$$Cc_i(A,u) = \int_0^u \frac{\cos W}{W}\cos u du = \ln\frac{W+u}{A} - \frac{1}{2}\left[Cin(W+u) - Cin(W-u)\right],$$

$$Sc(A,u) = \int_0^u \frac{\sin W}{W}\cos u du = \frac{1}{2}\left[Si(W+u) - Si(W-u)\right],$$

$$Cs(A,u) = \int_0^u \frac{\cos W}{W}\sin u du = \frac{1}{2}\left[Si(W+u) + Si(W-u)\right] - SiA,$$

$$Ss(A,u) = \int_0^u \frac{\sin W}{W}\sin u du = \frac{1}{2}\left[Cin(W+u) + Cin(W-u)\right] - CinA.$$

Here $W = \sqrt{u^2 + A^2}$, $Si(u) = \int\limits_0^u \frac{\sin u}{u} du$, $Cin(u) = \int\limits_0^u \frac{1-\cos u}{u} du$.

The expression for the slot current (5) completely determines the fields scattered by the slot in the intrinsic and extrinsic spaces, rectangular waveguide and half-space over an infinite plane. Hence, it allows us to obtain the electrodynamic characteristics of the waveguide-slot structure. Thus, the field reflection coefficient S_{11}, voltage standing wave ratio VSWR $= \frac{1+|S_{11}|}{1-|S_{11}|}$, and power radiation coefficient $|S_\Sigma|^2 = 1 - |S_{11}|^2$ can be easily defined. The expression for S_{11} can be written as

$$S_{11} = \left\{ 1 - \alpha \frac{16\pi\gamma(\cos^2\varphi) f(kL, \tilde{k}L)}{iabk^3[1-(\tilde{k}/k)^2]\{\sin 2kL + \alpha[2P_0(kd, 2kL) + W_0(kd, 2kL)]\}} \right\} e^{2i\gamma z}, \tag{7}$$

where

$$f(kL, \tilde{k}L) = 4 \sin kL \cos \tilde{k}L \frac{\sin kL \cos \tilde{k}L - (\tilde{k}/k) \cos kL \sin \tilde{k}L}{1 - (\tilde{k}/k)^2} - \sin 2kL \frac{\sin 2\tilde{k}L + 2\tilde{k}L}{2(\tilde{k}/k)},$$

$\gamma = \sqrt{k^2 - (\pi/a)^2}$ is the propagation constant of the H_{10}-wave.

The slot radiation field in the spherical coordinate system ρ, θ, ϕ (θ is the angle measured from the slot axis) contains the components H_ρ, H_θ, and E_ϕ. Here, only the electrical component will be presented in the form

$$E_\phi(\rho, \theta) = \frac{2ik^2 \sin\theta}{\omega} \int\limits_{-L}^{L} J(s) \frac{e^{-ikR(s)}}{R^2(s)} \left[1 + \frac{1}{ikR(s)} \right] \rho ds, \tag{8}$$

where $R(s) = \sqrt{\rho^2 - 2\rho s \cos\theta + s^2}$. In the far zone ($\rho \to \infty$, $\rho \gg 2L$), expression (8) determines the field radiation pattern $\bar{F}(\theta)$ of the slot radiator normalized to $F(\pi/2)$ which can be written as

$$\bar{F}(\theta) = \frac{\sin kL \cos qL \cos \tilde{k}L - \cos kL \left(\begin{array}{l} \dfrac{k^2 - \tilde{k}^2}{q^2 - \tilde{k}^2} \cos\theta \sin qL \cos \tilde{k}L \\ + \dfrac{k\tilde{k}}{q^2 - \tilde{k}^2} \sin^2\theta \cos qL \sin \tilde{k}L \end{array} \right)}{\sin\theta [\sin kL \cos \tilde{k}L - (k/\tilde{k}) \cos kL \sin \tilde{k}L]}, \tag{9}$$

where $q = k \cos\theta$.

The finite thickness h of the waveguide end wall can be taken into account by replacing $d \to d_e$ in formulas (5)–(8) using an approximate relation $d_e = d \exp(-\pi h/(2d))$ [13, 14], which is valid up to terms $\{(hd)/\lambda^2\}$ if the condition $(h/\lambda) \ll 1$ is fulfilled.

3. NUMERICAL AND EXPERIMENTAL RESULTS

The plots of the power radiation coefficient $|S_\Sigma|^2$ and phase of the reflection coefficient $\arg S_{11}$ [rad] as functions of the slot inclination angle φ are shown in Fig. 2. As can be seen, the Q-factor of the resonance curves increases, while the radiation coefficient decreases, as the slot axis in the waveguide cross-sectional plane is increased. When the angle φ is increased, the resonant slot wavelength λ_{res} determined by the equality $\arg S_{11} = 0$ [13] first shifts to the short-wavelength part of the wavelength range, and then, it increases starting from $\varphi \approx 30^\circ \div 40^\circ$. Thus, the slot lengthening or shortening as compared to the tuned slot length [13] can be observed. Note that the best waveguide matching with the slot is observed if the angle φ is small ($\varphi \approx 10^\circ$).

As can be seen, the plots in Fig. 3 allow us to trace how dispersion properties of the waveguide affect the structure of the diffraction characteristics. The slot is cut in the end wall of a rectangular waveguide along its diagonal. It can be seen that the slot resonates at different values of its electrical length $2L/\lambda$ depending on the operating wavelength λ.

The numerical simulation has shown that the angle φ does not significantly affect the parameters of the electromagnetic field radiated by the slot in the far and near zones. Typical curves of the field spatial distribution are shown in Fig. 4.

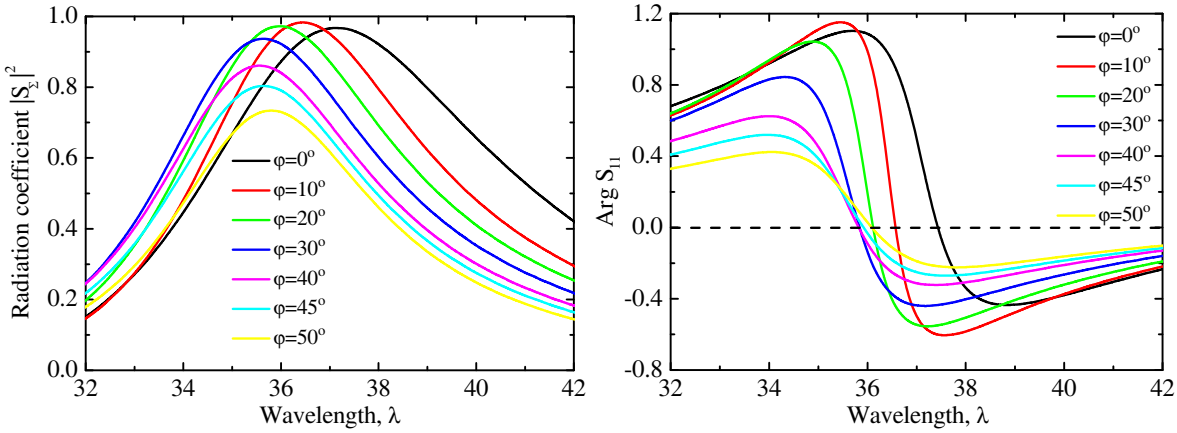

Figure 2. The radiation coefficient $|S_\Sigma|^2$ and phase of the reflection coefficient, arg S_{11} [rad], as wavelength λ [mm] functions. The radiator parameters: $\{a \times b\} = 23.0 \times 10.0\,\text{mm}^2$, $2L = 18.0\,\text{mm}$, $d/b = 0.1$, $h/a = 0.1$, $y_0/b = 0.5$.

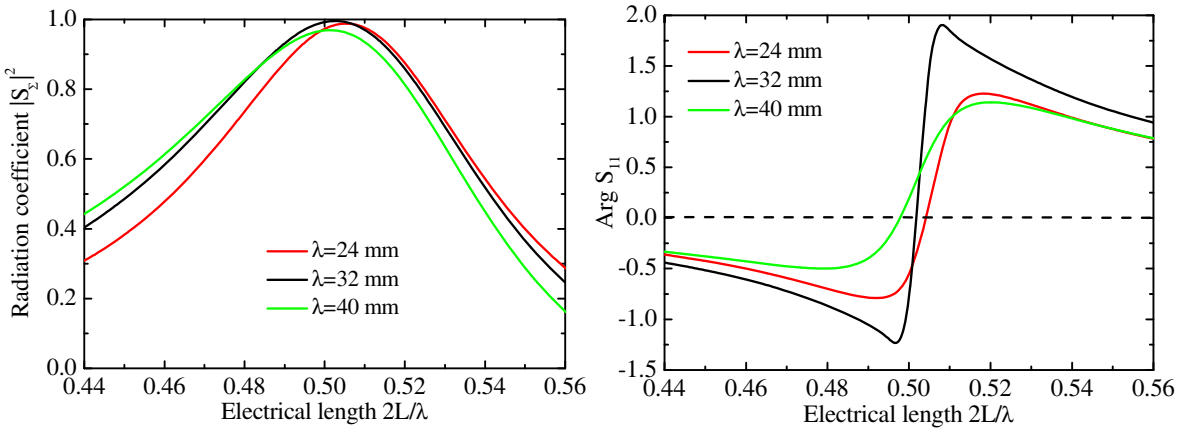

Figure 3. The radiation coefficient $|S_\Sigma|^2$ and phase reflection of the coefficient, arg S_{11} [rad], as electrical length functions. The radiator parameters: $\{a \times b\} = 23.0 \times 10.0\,\text{mm}^2$, $d/b = 0.1$, $h/a = 0.05$, $y_0/b = 0.5$, $\varphi = 23.5°$.

Good agreement of theoretical and experimental data shown in Fig. 6 allows us to conclude that the proposed approach to the diffraction problem solution is valid (the experimental model of the radiator is shown in Fig. 5). It also confirms the sufficient accuracy of the formulas used in the simulation. Slight differences between the theoretical and experimental values of the VSWR are explained by the fact that an approximate analytical method was used to solve the problem.

4. RADIATION OF A SLOT INTO HALF-SPACE ABOVE THE IMPEDANCE PLANE

In modern practice, projects to create new models of mobile objects allowing to reduce levels of reflected electromagnetic fields are being actively promoted. One of the main methods of reducing the field level scattered by objects in the microwave and EHF ranges consists in using coatings made of natural and artificial radio-absorbing materials, including metamaterials [15]. In this case, non-protruding slotted structures are often used as antennas. One alternative to radio-absorbing coatings can be slot impedance loads [16] consisting of slotted elements cut into the screen and strip conductors located in the slot

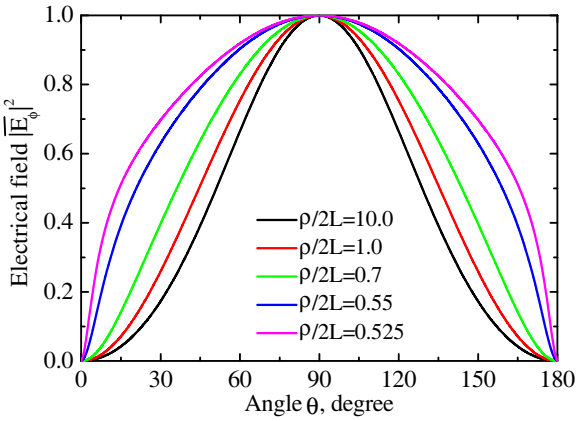

Figure 4. The spatial distributions of the slot radiation field $|\bar{E}_\phi(\rho,\theta)|^2$: $2L/\lambda = 0.51$, $2L = 18.0\,\text{mm}$, $\varphi = 45°$, $d/b = 0.1$, $h/a = 0.05$.

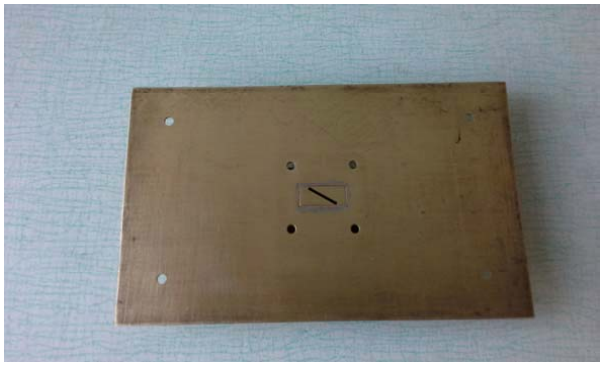

Figure 5. The experimental layout of the radiator.

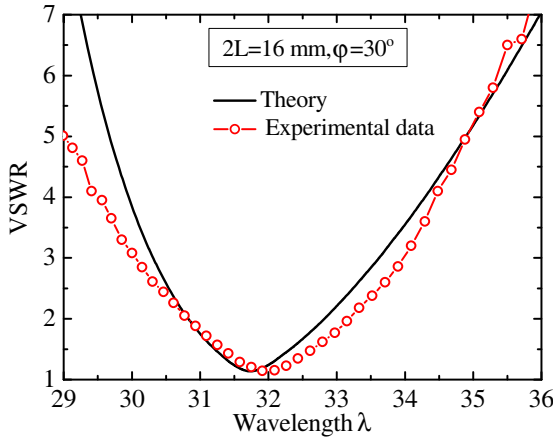

Figure 6. The theoretical and experimental VSWR curves as wavelength $\lambda\,[\text{mm}]$ functions: $\{a \times b\} = 23 \times 10\,\text{mm}^2$, $d = 1.5\,\text{mm}$, $h = 2.0\,\text{mm}$, $y_0 = b/2$.

apertures. In contrast to absorbing coatings, the impedance loadings are connected to a local area of reflecting object surface whose sizes are much smaller than its characteristic dimensions. However, in any variants of the impedance loads using slots as their electrodynamic model aperture-type elements are used which radiate into the space above an infinite screen with extrinsic impedance distributed over its surface. It should be noted that formulas or algorithms for determining external surface impedances for various types of structural coatings are now known [17, 18].

Thus, the development of effective methods intended for analyzing the slot radiation into the half-space above the impedance plane is relevant and demanded. As is known, the effectiveness of mathematical modeling is determined by rigorous formulation and solution of the corresponding boundary value problems, the time required for computational algorithm execution, and minimum computer RAM needed. The effectiveness of the approach directly depends on the degree of algorithm working out. Bellow, a technique for the numerical-analytical solution of the problem concerning the thin rectilinear slot exciting the space above the impedance screen by the generalized method of induced magnetomotive forces (MMF) is presented. The technique allows us to find the asymptotic expression for the magnetic current in the slot using the Green's functions for the vector potentials in the half-space above the impedance plane.

4.1. Green's Functions for Half-Space over an Impedance Plane

Let us construct the Green's functions for vector potentials in free space above the impedance plane. Assume that the plane $\{x0y\}$ in the Cartesian coordinate system (x, y, z) is characterized by constant distributed impedance $\bar{Z}_S = Z_S/Z_0$ ($Z_0 = 120\pi$ [Ohm] is the impedance of free space). Based on the general postulates of the electrodynamics theory [17, 18], the components of the tensor Green's functions of electric $\hat{G}^e(\vec{r}, \vec{r}')$ and magnetic $\hat{G}^m(\vec{r}, \vec{r}')$ types for vector Hertz potentials can be written in the form:

$$
\begin{aligned}
G^{e(m)}_{xx}(\vec{r}, \vec{r}') &= \frac{1}{4\pi^2} \int\limits_{-\infty}^{\infty} \int\limits_{-\infty}^{\infty} e^{-ik_x(x-x')-ik_y(y-y')} f^{e(m)}_{\chi}(z, z') dk_x dk_y, \\
G^{e(m)}_{yy}(\vec{r}, \vec{r}') &= \frac{1}{4\pi^2} \int\limits_{-\infty}^{\infty} \int\limits_{-\infty}^{\infty} e^{-ik_x(x-x')-ik_y(y-y')} f^{e(m)}_{\chi}(z, z') dk_x dk_y, \\
G^{e(m)}_{zz}(\vec{r}, \vec{r}') &= \frac{1}{4\pi^2} \int\limits_{-\infty}^{\infty} \int\limits_{-\infty}^{\infty} e^{-ik_x(x-x')-ik_y(y-y')} h^{e(m)}_{\chi}(z, z') dk_x dk_y,
\end{aligned}
\tag{10}
$$

where $\chi^2 = k^2 - k_x^2 - k_y^2$, $k_{x(y)}$ are the wavenumbers, and $f^{e(m)}_{\chi}(z, z')$ and $h^{e(m)}_{\chi}(z, z')$ are unknown functions. In a special case, when field sources are located directly on the impedance plane, the functions $f^{e(m)}_{\chi}(z, z')$ can be unambiguously defined. This possibility is based on the fact that the boundary conditions of the impedance type [17, 18] are consistent both for surface currents and for the fields that they excite. Thus, the excitation currents on the impedance plane can be specified only as a ratio [3, 19–21] between the magnetic current $\vec{J}^m$ and equivalent electric current $\vec{J}^e$ related by the formula $\vec{J}^m = -\bar{Z}_S[\vec{n}, \vec{J}^e]$, where $\vec{n}$ is the normal to the surface directed inside the impedance coating. Taking into account this ratio and the impedance condition for the tangential field components $[\vec{n}, \vec{E}] = -\bar{Z}_S[\vec{n}, [\vec{n}, \vec{H}]]$ at any point on the outer plane surface $\{x0y\}$, the following relation can written:

$$
\begin{gathered}
\left[\frac{\bar{Z}_S(k^2 + \chi^2)}{k} + i\frac{d}{dz}\right] f^m_{\chi}(z, z') = i\frac{df^e_{\chi}(z, z')}{dz}\bigg|_{z=z'=0}, \\
f^e_{\chi}(z, z') = -\bar{Z}_S^2 f^m_{\chi}(z, z')\big|_{z=z'=0}.
\end{gathered}
\tag{11}
$$

From relations (11), it is not difficult to obtain expressions for the unknown functions in explicit form

$$
f^e_{\chi}(z) = -\bar{Z}_S^2 C_{\chi} e^{-i\chi z}, \quad f^m_{\chi}(z) = C_{\chi} e^{-i\chi z}, \tag{12}
$$

where $C_{\chi} = \frac{4\pi}{i\chi} \frac{\chi k(1+\bar{Z}_S^2)}{\chi k(1+Z_S^2) + Z_S(k^2+\chi^2)}$.

Then the components of the Green's functions can be represented as sums of two terms, the first of which is the Green's function of the half-space over perfectly conducting plane. These terms can be written as:

$$
\begin{aligned}
G^m_{xx}(x, y, z; x', y', 0) &= \frac{1}{4\pi^2} \int\limits_{-\infty}^{\infty} \int\limits_{-\infty}^{\infty} C_{\chi} e^{-ik_x(x-x')-ik_y(y-y')-i\chi z} dk_x dk_y \\
&= 2\frac{e^{-ik\sqrt{(x-x')^2+(y-y')^2+(z)^2}}}{\sqrt{(x-x')^2+(y-y')^2+(z)^2}} \\
&\quad + \frac{1}{4\pi^2} \int\limits_{-\infty}^{\infty} \int\limits_{-\infty}^{\infty} \left(C_{\chi} - \frac{4\pi}{i\chi}\right) e^{-ik_x(x-x')-ik_y(y-y')-i\chi z} dk_x dk_y,
\end{aligned}
\tag{13a}
$$

$$G^e_{yy}(x,y,z;x',y',0) = -\frac{\bar{Z}_S^2}{4\pi^2}\int\limits_{-\infty}^{\infty}\int\limits_{-\infty}^{\infty} C_\chi e^{-ik_x(x-x')-ik_y(y-y')-i\chi z}dk_x dk_y$$

$$= 2\frac{e^{-ik\sqrt{(x-x')^2+(y-y')^2+(z)^2}}}{\sqrt{(x-x')^2+(y-y')^2+(z)^2}}$$

$$-\frac{1}{4\pi^2}\int\limits_{-\infty}^{\infty}\int\limits_{-\infty}^{\infty}\left(\bar{Z}_S^2 C_\chi + \frac{4\pi}{i\chi}\right)e^{-ik_x(x-x')-ik_y(y-y')-i\chi z}dk_x dk_y. \qquad (13b)$$

The expressions (13a) and (13b) were derived by using the well-known identity

$$\frac{e^{-ik\sqrt{(x-x')^2+(y-y')^2+(z)^2}}}{\sqrt{(x-x')^2+(y-y')^2+(z)^2}} = \frac{1}{2\pi}\int\limits_{-\infty}^{\infty}\int\limits_{-\infty}^{\infty}\frac{e^{-ik_x(x-x')-ik_y(y-y')-i\chi z}}{i\chi}\,dk_x dk_y. \qquad (14)$$

The following should also be noted separately. First, Equations (13a) and (13b) have additive representations. Second, under the condition $\bar{Z}_S \to 0$, they transform into expressions for the Green's functions of perfectly conducting plane in Eq. (10). Third, the denominators of expressions (13) and the Green's functions obtained in [20, 21] coincide, up to notation. Fourth, in contrast to [20, 21] where an attempt was made to obtain the Green's functions of a hybrid type based on replacing the equivalent currents, while here the components of the Green's functions of the magnetic and electric types are separated. This approach allows us to avoid a methodological collision [20, 21] when the expressions for the additive Green's functions contain components of electromagnetic fields, which must be found using the same functions.

4.2. Problem Formulation and Its Solution in a General Form

Let extraneous sources of electromagnetic field $\vec{H}_0^{in}(\vec{r})$, in which $\vec{r}$ is the radius vector of the point (x_{in}, y_{in}, z_{in}) in the local coordinate system, be located in the inner area marked in Fig. 7 by the index *in*. A narrow rectilinear slot cut in the common wall radiates into a free half-space above an impedance plane marked by the index *ext.* The common wall thickness is h, and the slot length and width are $2L$ and d. Without the loss of generality let us assume that a longitudinal slot axis $\{0s\}$ is parallel to the axis $\{0x\}$, and its center is at the coordinate system origin ($x = 0$, $y = 0$, $z = 0$).

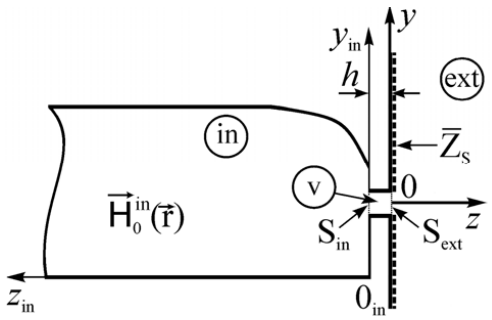

Figure 7. The radiation structure geometry and accepted notations.

The initial equation system can be written based on the continuity conditions for the tangential components of the total magnetic field at the coupling slot apertures S_{in} and S_{ext}. If the relation for the equivalent currents on the impedance surface, $J_x^m(s') = \bar{Z}_S J_y^e(s')$, is taken into account, the integral equation for the magnetic current in the slot can be written as (in contrast to Equation (1), which is

written at $\bar{Z}_S = 0$)

$$\left(\frac{d^2}{ds^2} + k^2\right) \int_{-L}^{L} J_x^m(s') \left[G_{xx}^{m(in)}(s,s') + G_{xx}^{m(ext)}(s,s')\right] ds'$$

$$+ik\bar{Z}_S \int_{-L}^{L} J_x^m(s') \frac{\partial}{\partial z} \tilde{G}_{yy}^{e(ext)}(s,s') ds' = -i\omega H_{0s}^{(in)}(s). \tag{15}$$

Here $H_{0s}^{(in)}(s)$ is the projection of extraneous field sources onto the slot axis; $G_{xx}^{m(in)}(s,s')$ are components of the quasi-one-dimensional magnetic tensor Green's functions $\hat{G}^m(\vec{r},\vec{r}')$ for the vector potential of the corresponding volumes; $G_{xx}^{m(ext)}(s,s') = G_{xx}^m(s,0,0;s',\frac{d_e}{4},0)\frac{\partial}{\partial z}\tilde{G}_{yy}^{e(ext)}(s,s') = \frac{\partial}{\partial z}G_{yy}^e(s,0,z;s',\frac{d_e}{4},0)|_{z=0}$ are obtained from formulas (13a) and (13b) by substituting $z = 0$ after taking the derivative.

If the slot is excited by an arbitrary field $H_{0s}(s) = H_{0s}^s(s) + H_{0s}^a(s)$, i.e., if the slot center is displaced from the point $x = a/2$, the magnetic current can be presented by symmetric and antisymmetric components marked by the indices s and a

$$J_x^m(s) = J_0^s f^s(s) + J_0^a f^a(s), \tag{16}$$

where $J_0^{s(a)}$ are the unknown complex amplitudes. If Eq. (16) is substituted into Eq. (15) at $\bar{Z}_S = 0$, the unknown amplitudes can be obtained as the ratios of the corresponding components of the magnetomotive force to the sum of the slot intrinsic $Y_{s(a)}^{(in)}(kd_e, kL)$ and extrinsic $Y_{s(a)}^{(ext)}(kd_e, kL)$ conductivities for a perfectly conducting plane [19]. The expression for the additional component to the partial extrinsic slot conductivities, $(Y_{s(a)}^{(ext)}(kd_e,kL) = Y_{s(a)}^{(ext)}(kd_e,kL)\Big|_{\bar{Z}_S=0} + \Delta Y_{s(a)}^{(ext)}(kd_e,kL))$, can be easily obtained by taking into account the structure of the Equation (15) and represent the Green's functions of the outer region as two-component sums in Eq. (13). This expression can be written as

$$\Delta Y_{s(a)}^{(ext)}(kd_e,kL) = \frac{\bar{Z}_S}{2\pi i} \int_{-L}^{L} f^{s(a)}(s) \int_{-L}^{L} f^{s(a)}(s')$$

$$\times \int_{-\infty}^{\infty}\int_{-\infty}^{\infty} \frac{\chi^2k^2(1+\bar{Z}_S^2) - (k^2+\chi^2)(k^2-k_x^2)}{\chi^2k^2(1+\bar{Z}_S^2) + \bar{Z}_S(k^2+\chi^2)\chi k} e^{-ik_z(s-s')-ik_x(d/4)} dk_x dk_z ds' ds. \tag{17}$$

Under the condition $|\bar{Z}_S^2| \ll 1$, expression (17) can be simplified

$$\Delta Y_{s(a)}^{(ext)}(kd_e,kL)\Big|_{|\bar{Z}_S^2|\ll 1} = \frac{\bar{Z}_S}{2\pi i} \int_{-L}^{L} f^{s(a)}(s) \int_{-L}^{L} f^{s(a)}(s')$$

$$\times \int_{-\infty}^{\infty}\int_{-\infty}^{\infty} \frac{\chi^2k^2 - (k^2+\chi^2)(k^2-k_x^2)}{\chi^2k^2 + \bar{Z}_S(k^2+\chi^2)\chi k} e^{-ik_z(s-s')-ik_x(d/4)} dk_x dk_z ds' ds. \tag{18}$$

If the slot is symmetrically excited under the condition $\varphi = 0°$, the basis function can be determined by the formula $f^s(s) = (\cos ks - \cos kL)$. Then according to Eq. (5), the additional term to the external conductivity can be presented as

$$\Delta Y^{(ext)}(kd_e,kL) = \frac{2\bar{Z}_S}{\pi i} \int_{-\infty}^{\infty}\int_{-\infty}^{\infty} \left\{ \begin{array}{l} \dfrac{\chi^2k^2(1+\bar{Z}_S^2) - (k^2+\chi^2)(k^2-k_x^2)}{\chi^2k^2(1+\bar{Z}_S^2) + \bar{Z}_S(k^2+\chi^2)\chi k} \\ \times \left[\dfrac{kk_x \sin kL \cos k_xL - k^2 \cos kL \sin k_xL}{(k^2-k_x^2)k_x}\right]^2 e^{-ik_z(d_e/4)} \end{array} \right\} dk_x dk_z, \tag{19}$$

which, under condition $|\bar{Z}_S^2| \ll 1$, converts to the following expression

$$\Delta Y^{(ext)}(kd_e, kL) = \frac{2\bar{Z}_S}{\pi i} \int\limits_{-\infty}^{\infty} \int\limits_{-\infty}^{\infty} \left\{ \begin{array}{l} \dfrac{\chi^2 k^2 - (k^2+\chi^2)(k^2-k_x^2)}{\chi^2 k^2 + \bar{Z}_S(k^2+\chi^2)\chi k} \\ \times \left[\dfrac{k k_x \sin kL \cos k_x L - k^2 \cos kL \sin k_x L}{(k^2-k_x^2)k_x} \right]^2 e^{-ik_z(d_e/4)} \end{array} \right\} dk_x dk_z. \tag{20}$$

As can be seen from formulas (17)–(20), the additional component to the external conductivity of the slot cut in the impedance plane can be expressed as the double infinite integrals over the frequency parameters k_x and k_z. Its value depends on the impedance $\bar{Z}_S$ which can significantly affect the slot radiation coefficient. As expected, if the plane is perfectly conducting ($\bar{Z}_S = 0$), additional component $\Delta Y^{(ext)}(kd_e, kL) = 0$.

4.3. Boundedness of the Integral Equation Kernel for a Current

Without the loss of generality, let us numerically estimate the boundedness of the integral equation kernel (15) for the magnetic Green's function specified by expression (13a). Based on formulas (13a) and (14) under the condition ($x = x', y = y', z = 0$), the following expression can be obtained

$$G_{xx}^m = -\frac{1}{\pi} \int\limits_{-\infty}^{\infty} \int\limits_{-\infty}^{\infty} \frac{ik(1+\bar{Z}_S^2)}{\chi k(1+\bar{Z}_S^2) + \bar{Z}_S(k^2+\chi^2)}\, dk_x dk_y. \tag{21}$$

On the complex k_x and k_y planes, the integration paths in formula (21) should pass along the real axes from $-\infty$ to $+\infty$ so that the integrand branch points passed around them in semicircles of infinitely small radiuses. The conditional intervals $-k_{x\,\min}; +k_{x\,\min}$ and $-k_{y\,\min}; +k_{y\,\min}$ including these singular points should be single out in the integration contours. Since the integrand in Eq. (21) is an even function with respect to k_x and k_y, the integral can be define as a sum

$$\begin{aligned} G_{xx}^m \;=\; & -\frac{1}{\pi} \int\limits_{-k_{x\,\min}}^{k_{x\,\min}} \int\limits_{-k_{y\,\min}}^{k_{y\,\min}} \frac{ik(1+\bar{Z}_S^2)}{\chi k(1+\bar{Z}_S^2) + \bar{Z}_S(k^2+\chi^2)}\, dk_x dk_y \\ & -\frac{2}{\pi} \int\limits_{k_{x\,\min}}^{\infty} \int\limits_{k_{y\,\min}}^{\infty} \frac{ik(1+\bar{Z}_S^2)}{\chi k(1+\bar{Z}_S^2) + \bar{Z}_S(k^2+\chi^2)}\, dk_x dk_y. \end{aligned} \tag{22}$$

Thus, the two-dimensional integral in Eq. (21) can be represented by the sum of two integral terms in Eq. (22): the first is a definite integral, hence, it is bounded for any arbitrarily wavelength λ, while the convergence of the second term (improper integral) determines the boundedness of the modulus G_{xx}^m. Therefore, the correct calculation of a definite integral cannot be discussed here.

In the simulation, it was assumed that $k_{x\,\min} = k_{y\,\min} = k - k \cdot 10^{-6}$ and $\lambda = 0.03\,\text{m}$. The infinite integration limits in Eq. (21) were replaced by the finite limits $k_{x\,\max} = k_{y\,\max} = k_{\max}$. The obtained moduli of improper integrals multiplied by a coefficient $4\pi^2$ are summarized in Table 1 as the function of $k_{\max}$ and real impedances $\bar{Z}_S$.

Table 1. Modulus of the improper integrals.

$\bar{Z}_S \backslash k_{\max}$	$k_{\max} = k \cdot 10^3$	$k_{\max} = k \cdot 10^6$	$k_{\max} = k \cdot 10^9$	$k_{\max} = k \cdot 10^{12}$
$\bar{Z}_S = 0.0$	$4.6 \cdot 10^6$	$4.639 \cdot 10^9$	$4.639 \cdot 10^{12}$	$4.639 \cdot 10^{15}$
$\bar{Z}_S = 10^{-6}$	$4.6 \cdot 10^6$	$3.858 \cdot 10^9$	$2.973 \cdot 10^{10}$	$2.947 \cdot 10^{10}$
$\bar{Z}_S = 10^{-4}$	$4.587 \cdot 10^6$	$2.053 \cdot 10^8$	$4.868 \cdot 10^8$	$2.947 \cdot 10^8$
$\bar{Z}_S = 10^{-2}$	$1.151 \cdot 10^6$	$3.895 \cdot 10^6$	$2.948 \cdot 10^6$	$2.948 \cdot 10^6$

As can be seen from Table 1, in the case of a perfectly conducting plane ($\bar{Z}_S = 0$), the modulus of the improper integral is unbounded due to the behavior of Green's functions in the vicinity of the singular point $r = r'$. This situation changes radically when the surface impedance of the plane is finite ($\bar{Z}_S > 0$). In this case, the improper integral becomes conditionally convergent. Moreover, the higher $\bar{Z}_S$ is, the higher the rate of the integral convergence is. In any case, the modulus of the Green's function G^m_{xx} turns out to be bounded if impedance $\bar{Z}_S$ is not zero. Note that the simulation results including those presented here for the Green's functions G^m_{xx} and G^e_{yy} carried out with a wide variation of the input parameters have led to the same conclusion. That is, the Green's functions G^m_{xx} and G^e_{yy} can be calculated with any predetermined accuracy. Therefore, it follows from the obtained numerical estimates that if the parameter $\bar{Z}_S$ is finite, the Green's functions (13a) and (13b) are regularized functions, and the integral equation (15) is the regularized integral equation.

5. CONCLUSION

In the paper, the approximate analytical expressions defining the slot current distribution function and fields radiated by the slot can be useful not only for multivariate analysis of the electrodynamic characteristics of the antenna-waveguide structures, but also in combination with other methods, for simulating multielement radiating systems, using a narrow oblique slot cut in an end wall of a semi-infinite rectangular waveguide.

The problem of slot radiating into a half-space over an infinite impedance plane was solved by a generalized method of induced MMF for arbitrary slot excitation modes and intrinsic region types. To determine the excitation currents related by the impedance condition at the slot aperture, the Green's functions for the half-space over the perfectly conducting plane were used. The Green's functions were previously constructed as sums of two terms, one of which is the Green's function for the half-space over the perfectly conducting plane. Thus, the effect of the impedance plane coating upon the slot characteristics was mathematically reduced to including an additional term in the formula for the external conductivity of the slotted element. This technique allows us to use as basis functions problem solutions obtained for a slot radiating into a space above a perfectly conducting plane including solutions which have already become classical. Expressions for the additional terms to the external slot conductivity were obtained in a closed form. However, simulation by using these terms is associated with some difficulties concerning the improper integrals calculated on the complex wavenumber plane.

REFERENCES

1. Schaik, H. J., "The performance of an iris-loaded planar phased-array antenna of rectangular waveguides with an external dielectric sheet," *IEEE Trans. Antennas Propag.*, Vol. 26, 413–419, 1978.
2. Harrington, R. F. and J. R. Mautz, "Computational methods for transmission of waves," *Electromagnetic Scattering*, Uslenghi P. L. E. (ed.), 429–470, Academic Press, NY, 1978.
3. Nesterenko, M. V. and Yu. M. Penkin, "Diffraction radiation from a slot in the impedance end of a semi-infinite rectangular waveguide," *Radiophysics and Quantum Electronics*, Vol. 47, 489–499, 2004.
4. Das, B. N., A. Chakraborty, and N. V. S. Narasimna Sarma, "S matrix of slot-coupled H-plane Tee junction using rectangular waveguides," *IEEE Trans. Microwave Theory Tech.*, Vol. 38, 779–781, 1990.
5. Abdelmonem, A., H.-W. Yao, and K. A. Zaki, "Slit coupled E-plane rectangular T-junctions using single port mode matching technique," *IEEE Trans. Microwave Theory Tech.*, Vol. 42, 903–907, 1994.
6. Berdnik, S. L., V. A. Katrich, M. V. Nesterenko, and Yu. M. Penkin, "Waveguide T-junctions with resonant coupling between sections of different dimensions," *International Journal of Microwave and Wireless Technologies*, Vol. 9, 1059–1065, 2017.

7. Berdnik, S. L., V. A. Katrich, M. V. Nesterenko, Yu. M. Penkin, and O. M. Dumin, "Yagi-Uda combined radiating structures of centimeter and millimeter wave bands," *Progress In Electromagnetics Research M*, Vol. 93, 89–97, 2020.
8. Mazzarella, G. and G. Montisci, "Accurate modeling of coupling junctions in dielectric covered waveguide slot arrays," *Progress In Electromagnetics Research M*, Vol. 17, 59–71, 2011.
9. Montesions-Ortego, I., M. Sierra-Perez, M. Zhang, J. Hirokawa, and M. Ando, "Mutual coupling in longitudinal arrays of compound slots," *Progress In Electromagnetics Research B*, Vol. 46, 59–78, 2013.
10. Camacho, M., R. R. Boix, F. Medina, A. P. Hibbings, and J. R. Sambles, "Extraordinary transmission and radiation from finite by infinite arrays of slots," *IEEE Trans. Antennas Propag.*, Vol. 68, 581–586, 2020.
11. Yang, R. and A. S. Omar, "Analysis of thin inclined rectangular aperture with arbitrary location in rectangular waveguide," *IEEE Trans. Microwave Theory Tech.*, Vol. 41, 1461–1463, 1993.
12. Rud, L. A., "Axially rotated step junction of rectangular waveguides and resonant diaphragms based thereupon," *Telecommunications and Radio Engineering*, Vol. 55, 17–26, 2001.
13. Nesterenko, M. and V. Katrich, "The asymptotic solution of an integral equation for magnetic current in a problem of waveguides coupling through narrow slots," *Progress In Electromagnetics Research*, Vol. 57, 101–129, 2006.
14. Warne, L. K., "Eddy current power dissipation at sharp corners: closely spaced rectangular conductors," *Journal of Electromagnetic Waves and Applications*, Vol. 9, 1441–1458, 1995.
15. Lagarkov, A. N., V. N. Semenenko, A. A. Basharin, and N. P. Balabukha, "Abnormal radiation pattern of metamaterial waveguide," *PIERS Online*, Vol. 4, 641–644, 2008.
16. Koshkid'ko, V. G. and O. V. Alpatova, "The equivalent surface impedance slit impedance of the load based on the holes in the screen. The case of E-polarization," *Technology and Electronics*, Vol. 48, 57–63, 2003.
17. Tretyakov, S., *Analytical Modeling in Applied Electromagnetics*, Artech House, NY, 2003.
18. Nesterenko, M. V., V. A. Katrich, Yu. M. Penkin, S. L. Berdnik, and O. M. Dumin, *Combined Vibrator-slot Structures: Theory and Applications*, Springer Nature Swizerland AG, Cham, Swizerland, 2020.
19. Nesterenko, M. V., V. A. Katrich, Yu. M. Penkin, and S. L. Berdnik, *Analytical and Hybrid Methods in Theory of Slot-hole Coupling of Electrodynamic Volumes*, Springer Science+Business Media, NY, 2008.
20. Yoshitomi, K., "Equivalent currents for an aperture in an impedance surface," *IEEE Trans. Antennas Propag.*, Vol. 42, 1554–1556, 1994.
21. Yoshitomi, K., "Radiation from a slot in an impedance surface," *IEEE Trans. Antennas Propag.*, Vol. 49, 1370–1376, 2001.